Investigation of the nerve distribution pattern of leg muscles in rat

Tuncay Peker, Nadir Gülekon, Zafer Kutay Coşkun & Suna Ömeroğlu

Anatomical Science International

ISSN 1447-6959
Volume 88
Number 2

Anat Sci Int (2013) 88:83-90
DOI 10.1007/s12565-012-0169-3



Springer

Your article is protected by copyright and all rights are held exclusively by Japanese Association of Anatomists. This e-offprint is for personal use only and shall not be self-archived in electronic repositories. If you wish to self-archive your work, please use the accepted author's version for posting to your own website or your institution's repository. You may further deposit the accepted author's version on a funder's repository at a funder's request, provided it is not made publicly available until 12 months after publication.

Springer

Author's personal copy

Anat Sci Int
DOI 10.1007/s12565-012-0169-3

ORIGINAL ARTICLE

Investigation of the nerve distribution pattern of leg muscles in rat

Tuncay Peker · Nadir Gülekon · Zafer Kutay Coşkun · Suna Ömeroğlu

Received: 23 July 2012 / Accepted: 27 December 2012
© Japanese Association of Anatomists 2013

Abstract Information about the distribution of intramuscular nerve fibres within the skeletal muscles will enhance the understanding of their morphological structure and functions. This study was designed to examine the entire intramuscular nerve distribution pattern in rat leg muscles. The tibialis cranialis, tibialis caudalis, extensor digitorum longus, flexor digitorum longus, gastrocnemius, peroneus longus and brevis muscles were dissected from origo and insertion points under a surgical microscope in seven rats. These skeletal muscles from right hindlimbs were stained with Sihler's stain. The diameter of extramuscular and major nerve branches, number of major and minor nerve branches and anastomoses were measured and photographed under a stereomicroscope. In addition, serial sections were obtained from the left hindlimb muscles with S100 immunohistochemical staining and transferred to the computer to reconstruct images. A significant difference was found between the gastrocnemius and tibialis caudalis ($p < 0.001$), flexor digitorum longus and tibialis caudalis ($p < 0.003$), and peroneus longus and tibialis caudalis ($p < 0.049$) with regard to the diameter of major branches. The gastrocnemius was significantly different from the flexor digitorum longus, peroneus longus, extensor digitorum longus, tibialis caudalis and tibialis cranialis with regard to the number of minor nerve branches ($p < 0.001$). Knowledge of the branching pattern and some key landmarks, such as the number and diameter of major and minor nerve branches and the number of anastomoses between the nerve branches of skeletal muscles, is helpful in surgical or therapeutic interventions and botulinum toxin injections in areas of high extramuscular and intramuscular nerve density.

Keywords Rat · Skeletal muscles · Sihler staining method · Intramuscular nerve distribution · Morphometry

T. Peker (✉) · N. Gülekon · Z. K. Coşkun
Department of Anatomy, Gazi University Faculty of Medicine, 06500 Beşevler, Ankara, Turkey
e-mail: tpeker@gazi.edu.tr

S. Ömeroğlu
Department of Histology and Embryology, Gazi University Faculty of Medicine, 06500 Beşevler, Ankara, Turkey

Introduction

The compartmentalized structures of mammalian muscles have been morphologically documented by anatomical, histological and histochemical criteria, such as the arrangement of the muscle fibres, distribution of muscle fibre composition and intramuscular nerve distribution pattern (English and Lettbetter 1982; Sanders et al. 1994). Sihler's stain and the reconstructed pattern determined by tracing images of the muscle from serial histological sections are expected to have wide applicability in the area of neuroanatomical research. It will be useful in tracing nerves such as major and minor nerve branches as well as in studying the neuromuscular compartments. In addition, it might also be useful for demonstrating differences in the neural supply throughout development and pathological conditions (Wu and Sanders 1992).

Advanced knowledge of the intramuscular nerve ramification in muscles is important for providing valuable data for surgeons who perform operations such as neuromuscular transplants, especially functional muscular compartment transfers and effective injection of neuromuscular blocking agents (Lee et al. 2004; Han et al. 2006). Nowadays, botulinum toxin injections are used in plastic surgery to improve the esthetic appearance of bulky calves.

Published online: 12 January 2013

Author's personal copy

Sheverdin et al. (2009) suggested that using areas with the highest density of extra- and intramuscular branches may improve the efficacy of botulinum toxin injections. Our study is intended to provide useful information to anatomists and clinicians on several aspects such as the intramuscular ramification pattern of nerves and the type of neural communications to understand the muscular exercise physiology and to divide the muscular compartment during neuromuscular transplant.

Materials and methods

Seven male Wistar rats were examined in this study. Mean weight of the rats was 220 ± 20 g, and all the rats were 2.5 months old. Ethical approval was granted by the Local Animal Ethics Committee of Gazi University Faculty of Medicine. Tibialis cranialis, tibialis caudalis, extensor digitorum longus, flexor digitorum longus, gastrocnemius, peroneus longus and brevis muscles (McLaughlin and Chiasson 1990) were dissected intact between the distal and proximal end points under a surgical microscope (Zeiss; OPMI Pico, Oberkochen, Germany). All the selected muscles were removed with their extramuscular nerve branches and photographed under the stereomicroscope (Olympus SZ, Japan). These skeletal muscles from the right hindlimbs were stained with Sihler's stain, whereas those from the left hindlimb muscles were stained with S100 immunohistochemical staining (DAKO Corp., Carpinteria, CA, USA). Serial histological sections 5 μm in thickness with 0.5-mm intervals were obtained from all muscles stained with S100. The sections were examined and evaluated under a light microscope (Leica DM 4000B, Germany), transferred to the computer through a CCD camera and numbered for 3D reconstruction.

Modified Sihler staining technique

Briefly, the rat leg muscles were fixed in 10 % un-neutralised formalin for at least 4 weeks and then macerated in 3 % potassium hydroxide solution for 3 weeks. During this period, the specimens gradually whitened. The well-macerated specimens were then transferred into Sihler's solution I (one part glacial acetic acid, one part glycerin and six parts 1 % aqueous chloral hydrate) for decalcification for a period of 2 weeks or more until they became transparent. The specimens were then put in Sihler's solution II (one part stock Ehrlich's acid haematoxylin, one part glycerin and six parts 1 % aqueous chloral hydrate) for staining for a period that could not exceed 4 weeks. When the specimens were stained a deep purple, they were transferred again into Sihler's I solution in order to be purified from the excess stain. This procedure was stopped when the muscles were light purple and the nerve fibres were dark blue. The specimens were put into a weak aqueous solution of lithium carbonate for 1 h to darken the colour of the nerves. Then, they were transferred into increasingly graded glycerin solutions (50%, 80 % and 100 % for 24 h in each grade) with a few thymol crystals for clearing the excess stain. Successfully stained specimens had dark blue nerves and translucent non-nervous tissues.

S100 immunohistochemical staining technique

Polyclonal rabbit anti-S100 is intended for use in immunocytochemistry. Dilution polyclonal rabbit anti-S100 (code no. Z 0311) can be used at a dilution of 1:400 when applied on formalin-fixed, paraffin-embedded sections and using 20-min heat-induced epitope retrieval in DakoCytomation Target Retrieval Solution (code no. S 1700) and 30-min incubation at room temperature with the primary antibody. S100 immunohistochemical staining was used to demonstrate Schwann cells (Hagen et al. 1986).

Three-dimensional reconstruction and modelling technique

Three-dimensional reconstruction software (Surfdriver v3.5, Kailua, HI, USA) was used, the contours were drawn around the nerves on each image semi-automatically, and finally all individual images were transferred to a single volume in such a way that when all images were overlapped, the contours of nerve branches generated the 3D reconstruction of the nerve branches. Computer-aided reconstruction images were produced by using both Surfdriver and Cinema 4D software (Cinema 4D v.11, Maxon Computer Inc., Newbury, CA, USA).

Morphometric and statistical analysis

The nerve branches are classified as follows: the nerve branch entering the muscle is called the extramuscular (main) nerve branch. The nerve branches subdividing from the extramuscular nerve after the entry into the muscle are called major nerve branches. Branches subdividing from major nerve branches are called minor nerve branches.

Images taken under the stereomicroscope from muscles stained with Sihler's stain were transferred from a CCD camera to a personal computer to measure extramuscular, major and minor nerve branches. Measurements were obtained using Olympus DP2-BSW software (Olympus, Japan). The number of neural connections between different nerves was counted manually within a given region under a stereomicroscope.

Author's personal copy

Statistical analyses

One-way ANOVA analysis of variance was used to compare the nerve distribution of skeletal muscles. The Bonferroni test was used as the post hoc test.

Results

Measurements were performed to determine the number of extramuscular, major and minor nerve branches; the diameter of the extramuscular and major nerve branches; and the number of neural connections between different nerves. Data are shown in Tables 1 and 2.

Gastrocnemius

Two extramuscular nerve branches originated from the tibial nerve entering into both heads of the muscle from the proximal third. The thicker one innervated the bigger head of the muscle. Major branches entered the muscle in an almost vertical direction, then coursed in the cranial and caudal directions from the origin to insertion (Fig. 1a, b). The number of major nerve branches in the gastrocnemius muscle was between 4 and 10 (mean 6.29 ± 2.1), whereas the number of minor nerve branches was between 3 and 13 (mean 4.71 ± 3.63). The number of neural communications in the same muscle was between 6 and 13 (mean 8.29 ± 2.36) (Table 2). The types of neural communications were Y-, I- or U-shaped, with the majority being Y type. Neural communication intensity was found to be higher in the middle third of the muscle (Fig. 1a).

Peroneus longus and brevis

The superficial peroneal nerve coursed along between the peroneus longus and brevis muscle after giving main branches to these muscles. The main branch entering the peroneus longus was thicker than the main branch of the peroneus brevis, and it divided into two major branches that run until the distal part of the muscle, including the tendinous part (Fig. 2a, b). The main branch entering the peroneus brevis divided into three major branches. The thinner one innervated the proximal third of the muscle, whereas the middle major branch dispersed into the middle third. The third major branch was thicker and longer than the others and ran until the junction of the middle and distal third of the muscle (Fig. 2a, b). Minor nerve branches originating from the major one divided into 5 to 18 with a mean of 11.14 ± 5.08 (Table 2). The number of

Table 1 Distribution of the diameters of extramuscular (main) and major nerve branches in rat leg muscles

Muscles	*n*	Mean (μm)	±SD	Min. (μm)	Max. (μm)
Diameters of extramuscular nerve branches					
Gastrocnemius	20	172.81	69.61	63.30	316.50
Flexor digitorum longus	17	131.63	48.71	31.65	253.20
Peroneus longus and brevis	14	138.81	60.13	31.65	269.03
Extensor digitorum longus	16	115.72	39.00	63.30	189.90
Tibialis caudalis	17	115.43	39.31	31.65	189.90
Tibialis cranialis	15	123.86	61.14	25.32	221.55
Total	99	134.44	57.16	25.32	316.50
Diameters of major nerve branches					
Gastrocnemius	44	82.94	32.78	31.65	158.25
Flexor digitorum longus	32	80.12	27.01	34.82	129.77
Peroneus longus and brevis	32	73.79	34.33	18.99	189.90
Extensor digitorum longus	29	64.72	23.83	22.16	110.78
Tibialis caudalis	37	51.68	27.24	13.13	126.60
Tibialis cranialis	30	71.02	36.74	13.13	158.25
Total	204	71.05	32.26	13.13	189.90

Table 2 Distribution of the number of major and minor nerve branches and number of communications in rat leg muscles

Muscles	*n*	Mean	±SD	Min.	Max.
Number of major nerve branches					
Gastrocnemius	7	6.29	2.1	4.00	10.00
Flexor digitorum longus	7	4.57	1.62	2.00	7.00
Peroneus longus and brevis	7	4.57	1.81	2.00	7.00
Extensor digitorum longus	7	4.14	1.1	3.00	6.00
Tibialis caudalis	7	5.29	1.5	3.00	7.00
Tibialis cranialis	7	4.29	1.1	2.00	5.00
Number of minor nerve branches					
Gastrocnemius	7	4.71	3.63	3.00	13.00
Flexor digitorum longus	7	10.57	1.90	8.00	14.00
Peroneus longus and brevis	7	11.14	5.08	5.00	18.00
Extensor digitorum longus	7	20.14	8.00	12.00	30.00
Tibialis caudalis	7	13.57	3.10	10.00	18.00
Tibialis cranialis	7	12.00	4.12	6.00	19.00
Number of communications					
Gastrocnemius	7	8.29	2.36	6.00	13.00
Flexor digitorum longus	7	5.86	2.54	3.00	10.00
Peroneus longus and brevis	7	8.14	4.34	3.00	14.00
Extensor digitorum longus	7	26.57	12.22	10.00	41.00
Tibialis caudalis	7	5.14	2.34	2.00	8.00
Tibialis cranialis	7	4.57	1.40	3.00	7.00

Author's personal copy

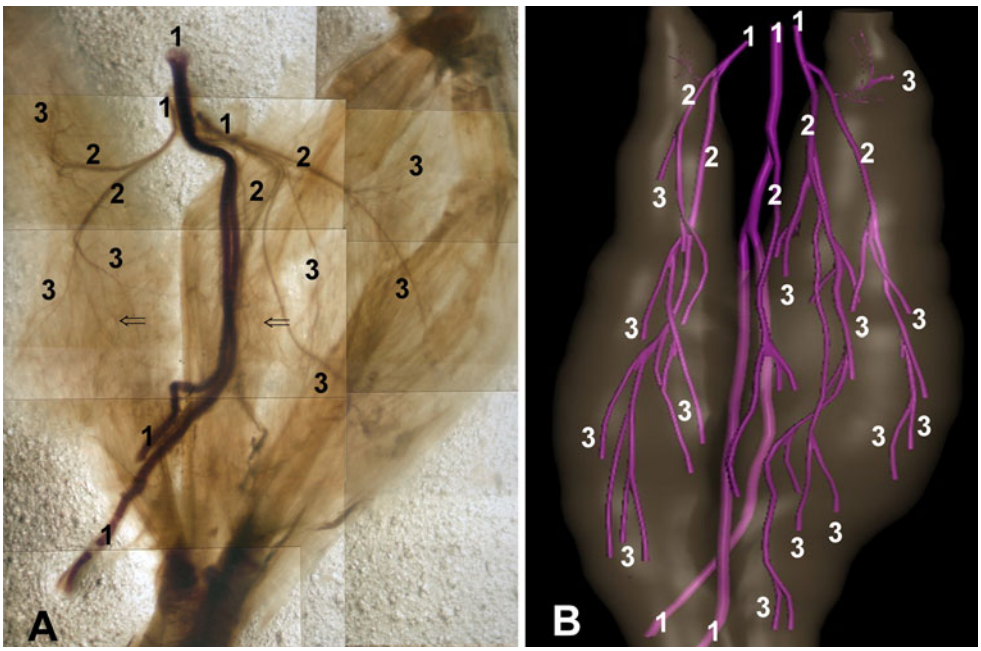


Fig. 1 General view of the gastrocnemius muscle. **a** Sihler's stain; **b** 3D reconstruction. Note the tibial nerve course between the two heads of the muscle. Neural communication intensity was found to be higher in the proximal third of the muscle (*open arrows*). *1* Main (extramuscular) nerve branch, *2* major nerve branch, *3* minor nerve branch

anastomoses was a mean of 8.14 ± 4.34. All the anastomoses were Y-, I- or U-shaped, with none of the types having a majority. Neural communication intensity was found to be higher in the proximal third of the muscle (Fig. 2a). In images obtained with S100 immunohistochemical staining, the extramuscular nerve branches originating from the superficial peroneal nerve were shown before entering the peroneus longus and brevis muscles (Fig. 2c).

Flexor digitorum longus

The main branches emerged from the tibial nerve. One of the main branches divided into two major branches. These major branches dispersed into the middle and distal part of the muscle and extended to the end of the muscle (Fig. 3a, b). The thinner main branch divided into two major branches at the fusion point of the proximal third and middle third of the muscle and innervated the muscle until the tendinous part. Minor nerve branches intersected with the muscle fibres at an oblique angle (Fig. 3a). Anastomoses were found to be higher in the middle part of the flexor digitorum longus muscle, and they were mostly Y- and I-shaped (Fig. 3c, d).

Extensor digitorum longus

The muscle was innervated by the superficial peroneal nerve. Two main branches entered the muscle from its proximal third at a right angle to the muscle fibres, then the major branches intersected with the muscle fibres in an oblique direction, and finally the minor branches showed a parallel course to the muscle fibres until their tendinous part (Fig. 4a, b). The highest number of neural communications was found in the extensor digitorum longus muscle (mean 26.57 ± 12.22) when compared with the other muscles (Table 2). The types of neural communications were Y-, I- and U-shaped, with the majority being Y-type. We rarely observed O-shaped anastomoses in these muscles (Fig. 4c). The neural communications were higher in the proximal third, distal third and middle third of the muscle, respectively (Fig. 4a).

Tibialis caudalis

Two main branches originating from the tibial nerve entered into the muscle from the junction point of the proximal and middle thirds. One of the main nerves innervated the proximal part of the muscle, and the second one dispersed in the middle and distal part of the muscle (Fig. 5a, b). Anastomosing nerve fibres were located in general in the proximal part. Neural communications in this part of the muscle were strikingly between major branches (Fig. 5a). These communications showed an "I" shape. The neural communication intensity was found to be higher in the upper half of the muscle. Major and minor nerve branches could also be demonstrated with S100 stain (Fig. 5c).

Tibialis cranialis

The muscle was innervated by the deep peroneal nerve. The main nerve divided into two branches before entering about the top of the muscle. One of the main branches

Author's personal copy

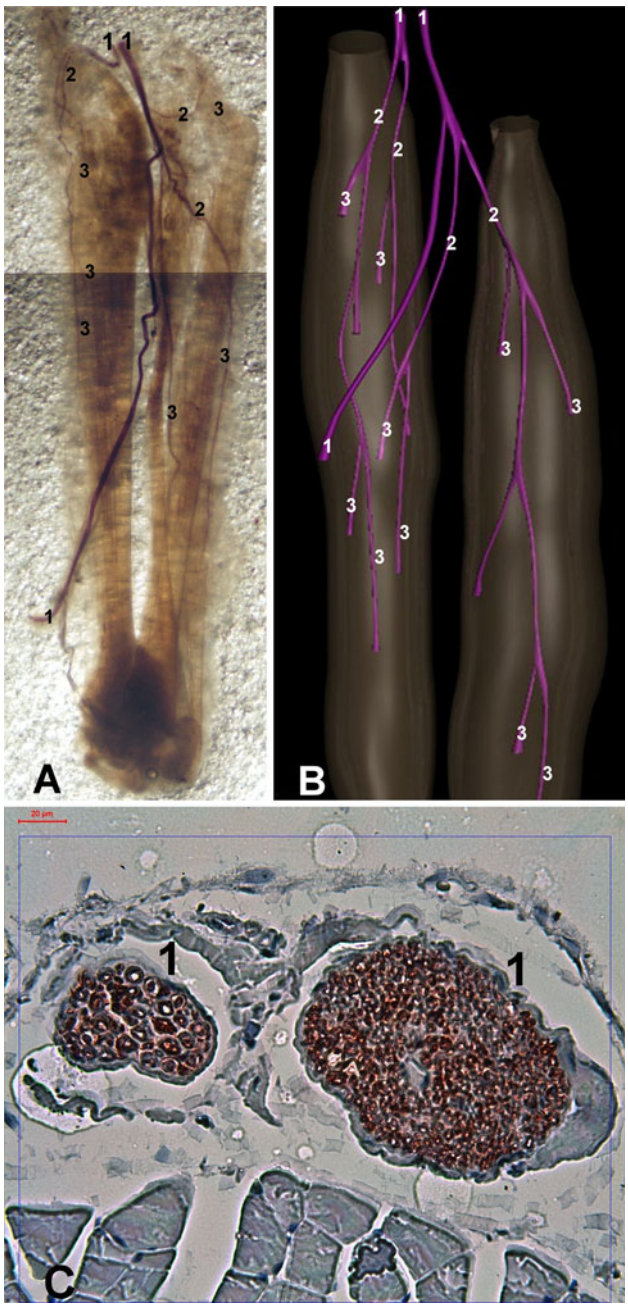


Fig. 2 General view of the peroneus longus and brevis muscles. **a** Sihler's stain; **b** 3D reconstruction. **c** Extramuscular nerve branches (*1*) originated from the superficial peroneal nerve before entering the peroneus longus and brevis muscles (S100 ×40). *2* Major nerve branch, *3* minor nerve branch

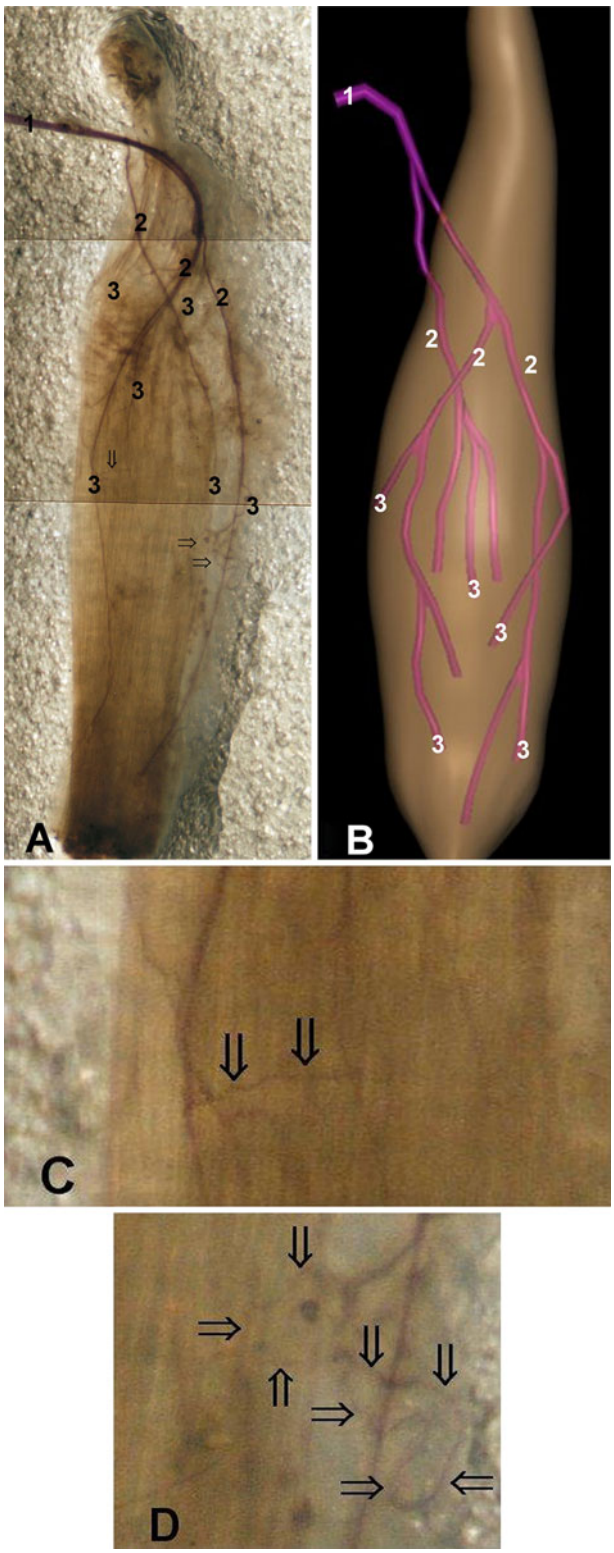


Fig. 3 General view of the flexor digitorum longus muscle. **a** Sihler's stain; **b** 3D reconstruction. **c**, **d** Magnification views of the middle third of the muscle. Note an I-shaped communication (**c**) and an O-shaped communication (**d**) between two different minor nerve branches (*open arrows*). *1* Main (extramuscular) nerve branch, *2* major nerve branch, *3* minor nerve branch

divided into two major branches that ran at the opposite borders of the muscle. The second one dispersed in the middle of the muscle. Minor nerve branches showed a parallel course in general (Fig. 6a, b). Neural anastomoses were located in the proximal part of the muscle with a majority having "Y" and "I" shapes.

Author's personal copy

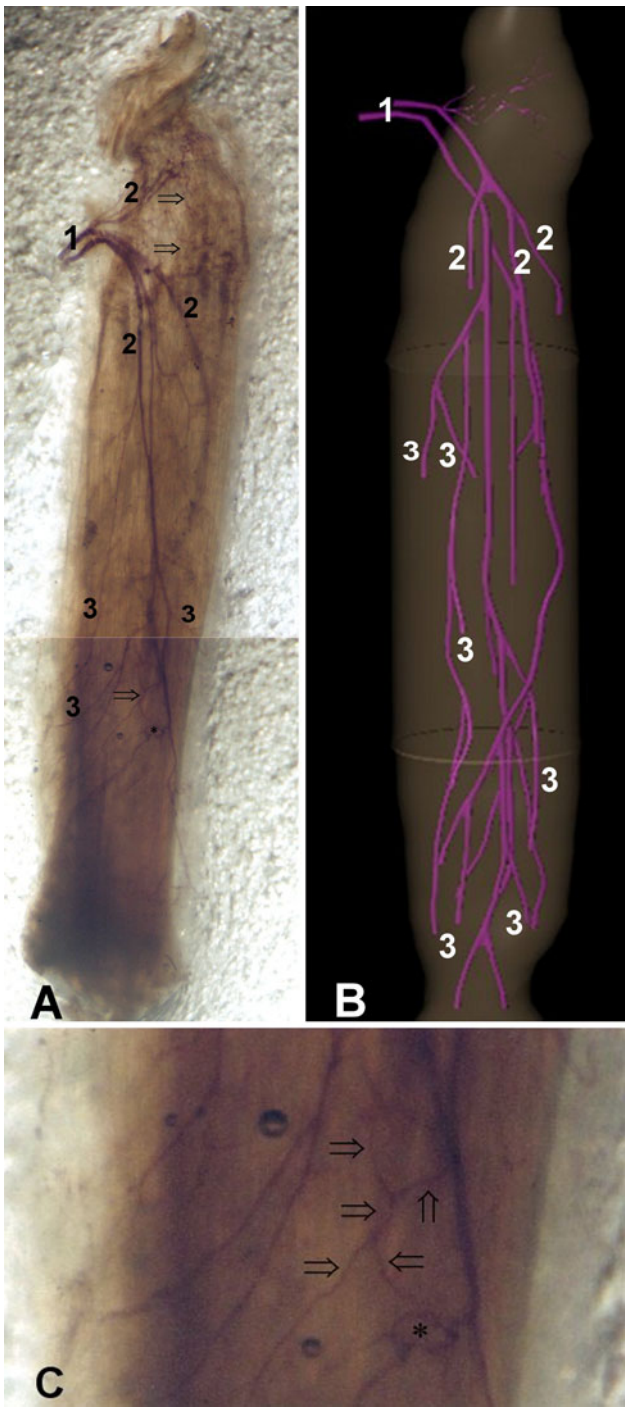


Fig. 4 General view of the extensor digitorum longus muscle. **a** Sihler's stain; **b** 3D reconstruction. The neural communications were higher in the proximal third, distal third and middle third of the muscle, respectively (*open arrows*). **c** Note a Y-shaped (*open arrows*) and O-shaped communication (*asterisk*) in the magnified view. *1* Main (extramuscular) nerve branch, *2* major nerve branch, *3* minor nerve branch

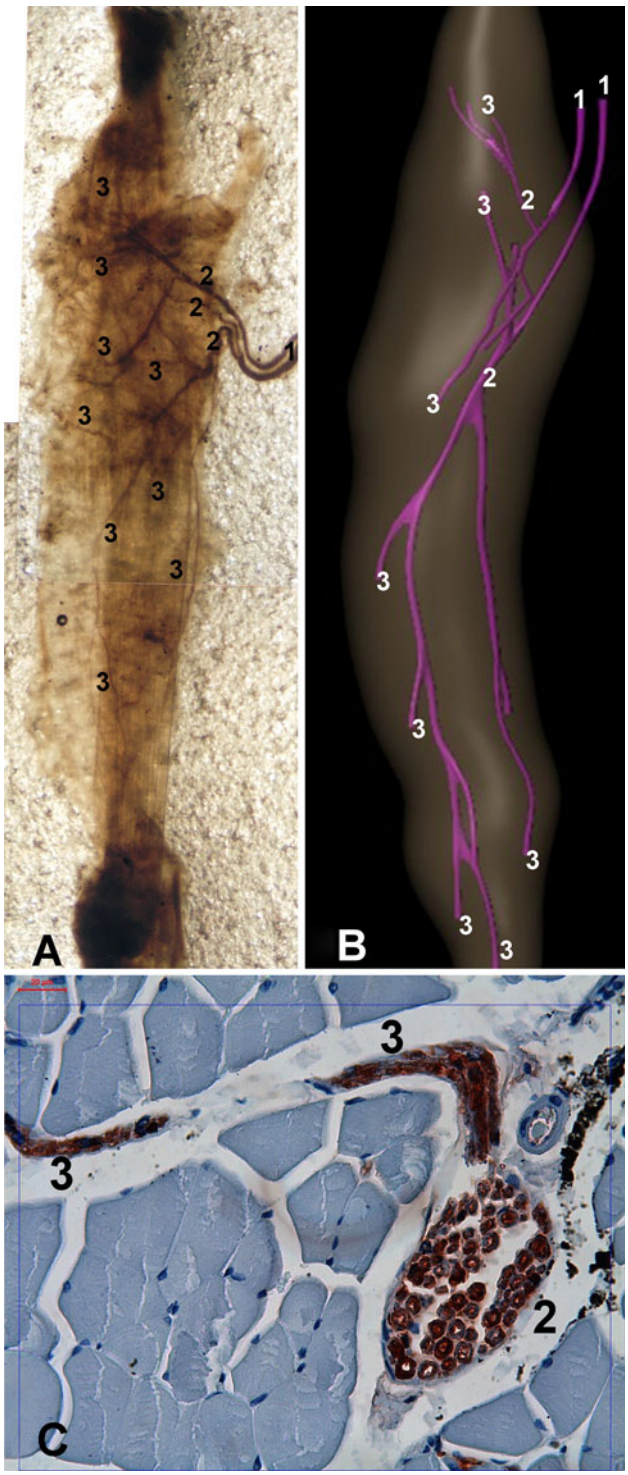


Fig. 5 General view of the tibialis caudalis muscle. **a** Sihler's stain; **b** 3D reconstruction. **c** Major nerve branch (*2*) and minor nerve branch (*3*) originating from the major branch at the ramification point are shown (S100 ×40). *1* Main (extramuscular) nerve branch

Statistical analysis

The gastrocnemius was different from the extensor digitorum longus ($p < 0.036$) and tibialis caudalis ($p < 0.029$), which were studied with regard to the diameter of the main branches. A significant difference was found between the gastrocnemius and tibialis caudalis ($p < 0.001$), flexor

Author's personal copy

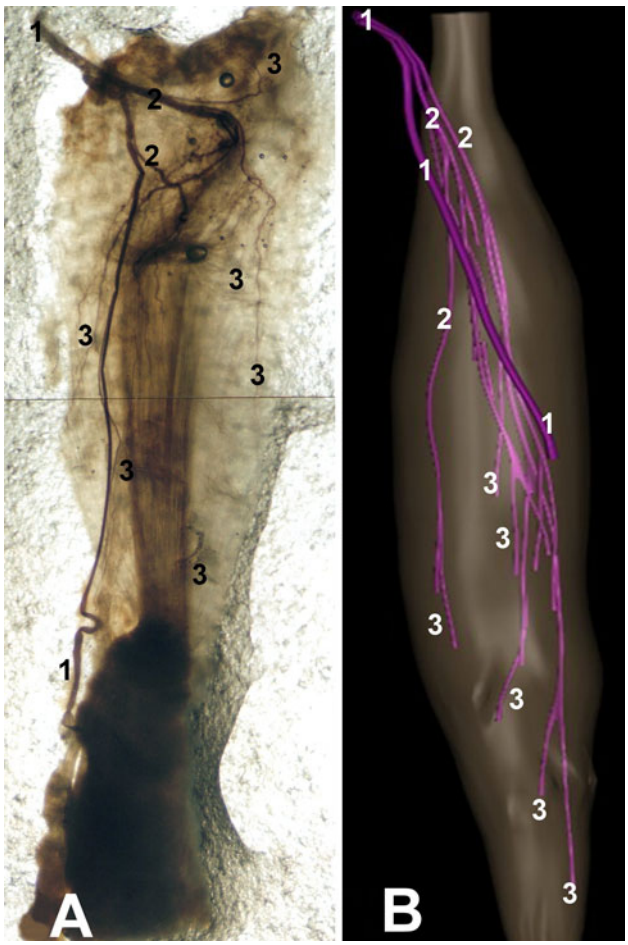


Fig. 6 General view of the tibialis cranialis muscle. **a** Sihler's stain; **b** 3D reconstruction. *1* Main (extramuscular) nerve branch, *2* major nerve branch, *3* minor nerve branch, *Double arrows* nerve communication, *asterisk* O-type nerve communication

digitorum longus and tibialis caudalis ($p < 0.003$), and peroneus longus and tibialis caudalis ($p < 0.049$) with regard to the diameter of major branches. The gastrocnemius was found to be significantly different from the flexor digitorum longus, peroneus longus, extensor digitorum longus, tibialis caudalis and tibialis cranialis with regard to the number of minor nerve branches ($p < 0.001$). The gastrocnemius, flexor digitorum longus and peroneus longus were significantly different from the extensor digitorum longus, tibialis caudalis and tibialis cranialis with regard to the number of neural anastomoses ($p < 0.001$).

Discussion

In the last decade, surgical procedures such as functioning free-muscle transfer and botulinum toxin injection have played an increasingly important role in plastic surgery. The efficacy and safety of these surgical procedures depend on sufficient knowledge of the extra- and intramuscular neurovascular distribution. Letbetter (1974) suggested that some muscles can be divided into several compartments, each one of which is supplied by one primary nerve branch. Each compartment had its identical muscle fibre orientation and unique sites of origin and ending that distinguished it from the other compartments. Muscles with two or more neurovascular compartments can be split into several units with independent functions, each of which has the potential to be used as a muscle flap with a neurovascular pedicle (Lim et al. 2006). Therefore, we investigated the nerve distribution and anastomosing pattern in rat leg muscles in the presented study. The flexor digitorum longus and tibialis cranialis had only one extramuscular nerve branch entering the muscle, while two extramuscular nerve branches entered the gastrocnemius, extensor digitorum longus, peroneus longus and brevis, and tibialis caudalis muscles. The highest number of major nerve branches was found in the gastrocnemius muscle, whereas the highest number of minor nerve branches was 20.14 ± 8.00 in the extensor digitorum longus. The tibialis caudalis, tibialis cranialis, flexor digitorum longus and peroneus longus muscles resembled each other in the number of minor nerve branches.

Liu et al. (1997) reported anastomoses between the branches of single nerves and of different nerves in the triceps muscle. They also reported that the communicating nerve fibres were Y-, I- or U-shaped. No standard anastomosis pattern was observed in different animals and different muscle groups. Peker et al. (2001) observed the same type of anastomotic relations between the nerve fibres in rabbit masticatory muscles. In addition to these, O-shaped communications between these branches were also observed (Peker et al. 2001). Similar to these findings, Gülekon et al. (2002) reported more than ten communicating branches in the distal part of all extraocular muscles. In the present study, all types of communicating nerve branches mentioned above were observed. We rarely observed O-shaped neural communications in rat leg muscles. In addition to this, the highest number of anastomoses was found in the extensor digitorum longus (mean 26.57 ± 12.22), whereas the least was found in the tibialis cranialis (4.57 ± 1.40). Knowledge about the density of anastomotic nerve branches is important in the field of functioning free-muscle transfer and botulinum toxin injection.

Liu et al. (1997) and Peker et al. (2001) observed that a few terminal nerve branches entered the tendons at the end of the muscle. In the present study, a few nerve fibres were observed to emerge from the distal portion of the nerve bundles terminating in the tendinous part of all skeletal muscles, especially the extensor digitorum longus and peroneus longus. In addition, the fewest nerve fibres found

Author's personal copy

in the tendinous part of the skeletal muscle were in the tibialis cranialis.

Computer-aided three-dimensional reconstruction techniques have been increasingly used. Gülekon et al. (2007) reported human foetal skeletal muscles using 3D reconstruction images on a computer. They reported that three-dimensional reconstruction images can fully show nerve branches as well as the detailed spatial relationships between branches, which is not possible with Sihler's staining and labelling. Three-dimensional reconstructed digital images of nerve branches can be rotated and displayed in any plane (x, y or z plane). Furthermore, these images can be used to create stereo and anaglyph images for 3D perception. In the present study, 3D reconstruction images from various rat leg muscles were obtained. Both methods proposed in this study successfully display the arrangement and relationship between extra- and intramuscular nerve branches, and the results achieved are consistent with each other.

In conclusion, we have examined the extra- and intramuscular nerves in the tibialis cranialis, tibialis caudalis, extensor digitorum longus, flexor digitorum longus, gastrocnemius, peroneus longus and brevis muscles in rats. Advanced knowledge of the intramuscular nerve distribution in a muscle will help surgeons to perform neuromuscular transplant surgery and effective botulinum toxin injection. In a future study, we hope that this study will guide further investigations in the field of nerve distribution in skeletal muscles.

Conflict of interest None.

References

English AW, Lettbetter WD (1982) Anatomy and innervation pattern of cat lateral gastrocnemius and plantaris muscles. Am J Anat 164:67

Gülekon N, Peker T, Liman F, Anil A, Turgut HB (2002) Demonstration of the nerve distribution of the extraocular muscles in rabbits (*Oryctolagus cuniculus*). Curr Eye Res 25(3): 179–188

Gülekon N, Peker T, Turgut HB, Anil A, Karaköse M (2007) Qualitative comparison of anatomical microdissection, Sihler's staining and computerized reconstruction methods for visualizing intramuscular nerve branches. Surg Radiol Anat 29(5): 373–378

Hagen EC, Vennegoor C, Schlingemann RO, Van der Velde EA, Ruiter DJ (1986) Correlation of histopathological characteristics with staining patterns in human melanoma assessed by (monoclonal) antibodies on paraffin sections. Histopathol 10:689–700

Han KH, Joo YH, Moon SE, Kim KH (2006) Botulinum toxin A treatment for contouring of the lower leg. J Dermatolog Treat 17:250–254

Lee HJ, Lee DW, Park YH, Cha MK, Kim HS, Ha SJ (2004) Botulinum toxin A for aesthetic contouring of enlarged medial gastrocnemius muscle. Dermatol Surg 30:867–871

Letbetter WD (1974) Influence of intramuscular nerve branching on motor unit organization in medial gastroenemius muscle. Anat Rec 178:402

Lim AY, Kumar VP, Sebastin SJ et al (2006) Split flexor carpi ulnaris transfer: a new functioning free muscle transfer with independent dual function. Plast Reconstr Surg 117:1927–1932

Liu J, Kumar VP, Shen Y, Lau HK, Pereira BP, Pho RW (1997) Modified Sihler's technique for studying the distribution of intramuscular nerve branches in mammalian skeletal muscle. Anat Rec 247(1):137–144

McLaughlin CA, Chiasson RB (1990) The muscular system, chap 3. In: Laboratory anatomy of the white rat, 3rd edn. McGraw-Hill, Boston, pp 23–50

Peker T, Turgut HB, Gülekon N, Anil A (2001) Demonstration of the nerve distribution of the masticatory muscles in rabbits (*Oryctolagus cuniculus*). Anat Histol Embryol 30(4):225–229

Sanders I, Wu BL, Mu L, Biller HF (1994) The innervation of the human posterior cricoarytenoid muscle: evidence for at least two neuromuscular compartments. Laryngoscopes 104:880

Sheverdin VA, Hur MS, Won SY, Song WC, Hu KS, Koh KS, Kim HJ (2009) Extra- and intramuscular nerves distributions of the triceps surae muscle as a basis for muscle resection and botulinum toxin injections. Surg Radiol Anat 31(8):615–621

Wu BL, Sanders I (1992) A technique for demonstrating the nerve supply of whole larynges. Arch Otolaryngol Head Neck Surg 118(8):822–827